



Research Article

A facile and low-cost route for producing a flexible hydrogel–PANI electrolyte/counter electrode applicable in dye-sensitized solar cells (DSSC)

Diego Oliveira Miranda^{1,2} · Matheus Figueiredo Dorneles¹ · Rodrigo Lambert Oréfice¹ 

Received: 7 August 2019 / Accepted: 8 November 2019 / Published online: 12 November 2019
© Springer Nature Switzerland AG 2019

Abstract

In this work, hybrid hydrogels were prepared based on poly(acrylic acid-co-acrylamide) hydrogels (Gel) and self-assembled nanostructured polyaniline (PANI). These hybrid hydrogels were prepared by in situ UV-assisted aniline polymerization during hydrogel network formation in a controlled interfacial reaction. They were then tested as flexible quasi-solid electrolytes with a counter electrode in dye-sensitized solar cells. This electrolyte-counter electrode system was prepared on top of a titanium dioxide layer deposited on a transparent and conductive anode electrode (ITO). Three different nanostructured Gel–PANI hybrid hydrogels were fabricated by employing different PANI concentrations and used for constructing electrolyte-counter electrode systems that displayed conductivities between 0.003 S/cm and 0.02 S/cm. Dye-sensitized solar cells (DSSC) that had the configuration ITO/TiO₂/Gel–PANI/ITO were prepared and tested using natural dye extracted from *Myrciaria cauliflora*. The energy conversion efficiency was evaluated under AM1.5 (100 mW/cm²) light irradiation and was found to reach values above 2.0%. The device's energy conversion efficiency was found to be higher than those of others with the same natural dye. The process proved to be fast and facile, and it utilized an inexpensive natural dye.

Keywords Solar cell · DSSC · *Myrciaria cauliflora* · Hydrogel · PANI

1 Introduction

Massive use of mobile devices and the spread of wearable technologies lead to constant searches for mobile power sources or sources incorporated into the devices. In this sense, flexible and low-cost solar cells can be widely employed due to the vast presence of energy radiated by the sun.

Dye-sensitized solar cells (DSSC), which are composed of a nanocrystalline semiconductor oxide film electrode, dye sensitizers, electrolytes, a counter electrode and a transparent conducting substrate, have the potential to develop low-cost photovoltaic (PV) devices. Like plants

that are effective in capturing energy over a wide range of light conditions, they work in lower light levels than do traditional PV. Thus, the outdoor environments of hospitals, airports, bus/train station windows and surfaces have become low cost energy sources [1].

Typically, dye-derived nanocrystalline titania (TiO₂) films have been used as photoanode, platinum-coated substrate as a counter electrode, and between them exists an electrolyte solution of I₃⁻/I⁻ in an organic solvent, forming sandwiched solar cells [2]. To reduce the tri-iodide ions of the liquid electrolyte, the counter electrode must have high electrocatalytic activity. In addition to platinum coating on transparent conductive oxide substrate, carbon is

✉ Rodrigo Lambert Oréfice, rorefice@demet.ufmg.br | ¹Department of Metallurgical and Materials Engineering, Universidade Federal de Minas Gerais (UFMG), Av. Antonio Carlos 6627, Belo Horizonte, MG 31270-901, Brazil. ²Instituto Federal de Educação, Ciência e Tecnologia de Minas Gerais (IFMG), Campus Sabará, Belo Horizonte, MG, Brazil.



usually used. Nevertheless, the high cost of platinum has triggered its replacement by other cheaper materials [3]. Conductive polymers, such as polyaniline (PANI), have been investigated as an alternative due to their properties including high conductivity, good stability, catalytic activity and low cost [4, 5].

Long-term operation of liquid electrolytes is usually restricted due to their sealing issues and volatility of the organic solvent. The development of quasi-solid-state electrolytes, such as gel structures, constitutes another approach to avoid the problems of liquid electrolytes. Conductive polymers such as PANI, polypyrrole, polythiophene, polyphenylene vinylene and polyacetylene are potential candidates for quasi-solid-state electrolytes [5].

DSSCs based on natural sensitizers (NDSSC) have become a topic of significant research because of their urgency and importance in the energy conversion field. Moreover, they offer advantages over more conventional approaches, such as easier fabrication, lower-cost and being constituted by nontoxic materials [6].

Anthocyanins are a viable alternative to red dyes from natural sources. They are soluble in water, which facilitates their incorporation into aqueous systems and may replace artificial red colorants such as Ponceau 4R, erythrosine and Bordeaux [7].

A good source of anthocyanin pigments is the fruit of the jaboticabeira. The jaboticaba (*Myrciaria cauliflora*) is a native Brazilian plant that is located mainly in several states of the southeastern region of the country [8]. As plants that are effective in capturing energy in a wide range of lighting conditions, dye-sensitized solar cells operate at lower light levels than traditional silicon solar cells.

The aim of this work was to develop a quasi-solid electrolyte with inside counter electrode based on an ionic hydrogel and PANI produced in one step over an ITO conductive glass substrate coated with TiO₂ nanoparticles, which were sensitized using natural dye from *Myrciaria cauliflora* as a photoactive electrode. Current density–voltage measurements were performed in darkness and under illumination conditions. Furthermore, the morphological, structural, electrical and thermal properties of the counter electrode were also investigated.

2 Materials and methods

2.1 Materials

Aniline was purchased from Merck. Acrylic acid (AA), polyethylene glycol diacrylate (Mw ~ 700 g mol⁻¹, PEGDA), acrylamide (AAM), 37% hydrochloric acid, ammonium persulfate, 2-hydroxy-2-methylpropiophenone (97%),

poly(vinyl alcohol) (Mw ~ 30,000 g mol⁻¹, 98% hydrolyzed, PVA), and titanium (IV) oxide nanopowder (primary particle size < 100 nm, ≥ 99.5% trace metals basis) were purchased from Sigma-Aldrich (St. Louis, MO, USA) and were used as received. Natural dye was extracted from the skin of *Myrciaria cauliflora*.

2.2 Construction of NDSSC-type solar cell

Poly(ethylene terephthalate) (PET) substrates coated with indium-doped tin oxide (ITO) (60 Ω/sq) with dimensions of 1 cm by 1.5 cm were used, in which one of the edges had a deposited aluminum contact of 2 mm, thus possessing an active area of 1.3 cm². They were previously washed with deionized water and with 2% neutral detergent, then heated to 50 °C for 1 h with moderate magnetic stirring. After rinsing with deionized water at the same temperature for 1 h, substrates were oven dried at 28 °C.

The substrates were then coated with titanium dioxide nanoparticles by preparing a slurry containing 1 g titanium dioxide nanoparticles and 0.3 g 99% acetic acid. The slurry was deposited on the substrate using a glass rod and dried at room temperature. The following procedures were used to produce hydrogel films on these substrates that will act as quasi-solid electrolyte with inside counter electrodes.

2.3 Synthesis of poly(acrylamide-co-acrylic acid) hydrogels

Hydrogels were prepared by formulating an aqueous solution with 77 wt% AA, 19 wt% AAm, 2 wt% PEGDA and 2 wt% photoinitiator. The final concentration of the reactants in water was 0.6 g ml⁻¹. The solution was then cast on glass slides and kept under ultraviolet radiation, using a light source consisting of three 8 W UVA lamps and a UVC lamp for 5 min. Samples were washed with water and dried under vacuum at room temperature to yield free standing hydrogel films.

2.4 Incorporation of PANI in the hydrogels by interfacial oxidative UV-assisted polymerization of aniline

Hydrogels containing PANI were prepared by combining two different solutions: (1) the first solution (solution A) was prepared following the same procedure described above. However, aniline was added in the final solution in concentrations of 2, 4 and 6 wt%, while an aqueous solution with a concentration of 1 mol L⁻¹ of HCl was used instead of pure water. (2) A second (solution B) solution was prepared by dissolving 12 wt% of PVA in a 1 mol L⁻¹ aqueous solution of HCl. Solution B was allowed to stir for

15 min. Thereafter, 2, 4 and 6 wt% ammonium persulfate (PANI initiator) were added to yield solutions with different concentrations of ammonium persulfate to match solutions A, which were prepared with 2, 4 and 6 wt% aniline, respectively. The obtained solutions were stirred vigorously for another 15 min.

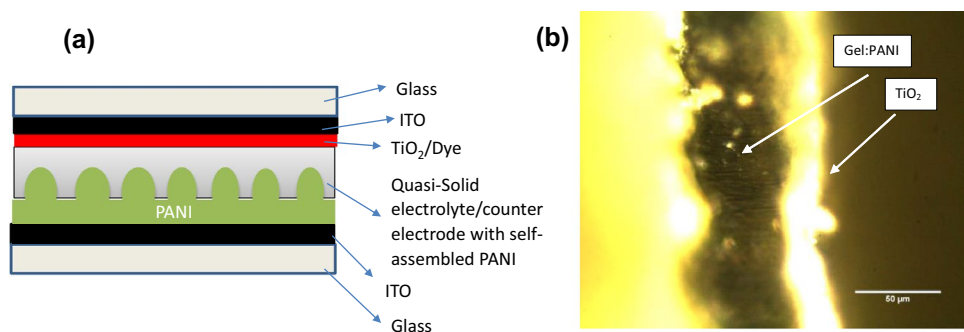
Solution B was placed on an ITO-PET substrate to yield a 1 mm thick film. After that, solution A was carefully poured over it. The visual initiation of the green-colored PANI formation at the interface between the two solutions was observed after 3 min of initial contact. The system was then photopolymerized by illuminating with the UV lamps. Free standing films of the hydrogels containing PANI were also obtained by repeating the same procedure described above on glass slides instead of ITO-PET substrates. These free standing films were used in the characterization procedures.

Table 1 shows aniline, water and monomer concentrations in solution A and the ammonium persulfate concentration in PVA solution (solution B).

Table 1 Concentrations of components (% w/w) in hydrogel precursor solution (solution A) and ammonium persulfate in PVA solution (solution B)

Sample	Hydrogel precursor solution (solution A) Concentration of the components (% w/w)			12 wt% PVA solution (solution B) Concentration of the components (% w/w)
	AA + AAM + PEGDA + Photoinitiator	H ₂ O	Aniline	
Gel:PANI 0	60	40	0	0
Gel:PANI 2	58	40	2	2
Gel:PANI 4	56	40	4	4
Gel:PANI 6	54	40	6	6

Fig. 1 **a** Scheme of the developed NDSSC with self-assembled PANI and **b** the corresponding SEM image



The dye was obtained by maceration of 100 g *Myrciaria cauliflora* (jabuticaba) bark and mixture with 100 ml ethanol. The obtained solution was kept at 5 °C for 24 h before vacuum filtration.

A Lugol solution consisting of 1 wt% iodine in equilibrium with potassium iodide (KI) in distilled water was used as the electrolyte. The dye solution was injected laterally into the TiO₂ film using a needle, while the electrolyte was injected through the surface of the gel. The cell was completed with another PET-ITO sheet and side sealing by hot pressing. The structure of the NDSSC and SEM image of the solar cell are shown in Fig. 1.

2.5 Characterization

2.5.1 Conductive atomic force microscopy (I-AFM)

AFM images were obtained by an AFM (Park Systems, Inc., XE-70) in conductive mode (I-AFM), which allows mapping of the surface of the samples by measuring the current flowing from the polarized sample in contact with a cantilever tip used as a probe. Since this current is of small magnitude, it is necessary to use a current amplifier before the image is processed. The DLCPA-200 external amplifier with variable gain adjustment between 103 and 1011 V coupled to the I-AFM Measurement Module was used.

2.5.2 Scanning electron microscopy (SEM)

Images of the surfaces of the films were obtained by scanning electron microscopy using a mini Sputter (PI Supplies-Sputter coater) system for their metallization and the JEOL JSM-6360LV and Quanta FEG 3D FEI scanning electron microscopes.

2.5.3 Differential scanning calorimetry (DSC)

DSC curves were obtained by using the EXSTAR DSC 7020 equipment. The DSC analyses were performed under a nitrogen atmosphere, with the first heating run starting

at $-20\text{ }^{\circ}\text{C}$ and ending at $130\text{ }^{\circ}\text{C}$, followed by a second run from -20 to $250\text{ }^{\circ}\text{C}$ with a rate of $10\text{ }^{\circ}\text{C}/\text{min}$.

2.5.4 Fourier transform infrared spectroscopy (FTIR) and UV-Vis spectroscopy

FTIR spectra of the samples were collected after keeping them dried in a vacuum oven at room temperature for 24 h. The attenuated total reflection technique (ATR) was employed, the accessory for which was coupled to the Thermo Scientific spectrophotometer model Nicolet 6700. UV-Vis spectra were collected by UV-2600 spectrophotometer, Shimadzu Corporation, Japan, model TCC-240A.

2.5.5 Nanoindentation

AFM nanoindentation measurements (Park Systems, Inc., XE-70) were performed to estimate the elastic modulus (E) of the gel-PANI films. The procedure involved printing a mark on the surface of the materials using the AFM cantilever, with a tip with known geometry employed as indenter. A constant tip shift velocity of $1\text{ }\mu\text{m}/\text{s}$ was used until the determined maximum force of $1.6\text{ }\mu\text{N}$ was reached and maintained constant for 0.5 s. Throughout the process, tip displacement was measured as a function of force. The nanoindentations of the films were performed by attaching free standing films of the gel-PANI onto a glass slide. AFM nanoindentation measurements were performed underwater so that the hydrogel-PANI samples could be studied in their full swollen state. The water used in the nanoindentation had $\text{pH}=7$ and resistivity of $1\text{ M}\Omega/\text{cm}$. Measurements were performed after a stabilization time underwater of 45 min. The procedure for estimating the elastic modulus from AFM nanoindentation measurements was developed by Oliver and Pharr [9] and is incorporated into Park Systems Corporation's XEI 1.8.9 software, which is used to obtain values of at least 30 nanoindentations per sample.

2.5.6 Conductivity measurement by the 4-point method

Free standing films of gel-PANI were submitted for analysis of their conductivity through the four-probe system, using a Keithley 2400 electrometer conjugated to the Signatone GMX45 four-point system.

The electrical conductivity of materials can be measured by the four-point technique, whose calculation of conductivity can be given by the relationship of Blythe and Bloor [10].

$$\sigma = \frac{0.221}{e.R} \quad (1)$$

where ' σ ' is the conductivity (S/cm), ' e ' corresponds to the sample thickness in centimeters (cm) and ' R ' corresponds to the electrical resistance of the sample in ohms (Ω).

2.5.7 Solar cell characterization

The cells were characterized by obtaining current versus voltage curves ($I \times V$) in the dark and under solar spectral irradiance of AM1.5 ($100\text{ mW}/\text{cm}^2$) using the combination of full spectrum LED lamps with sample temperature control at $25\text{ }^{\circ}\text{C}$. This equipment was calibrated using a calibrated commercial 10 W module. A circuit based in MOS-FET IRF 640 and controlled by the National Instruments myDAQ system was used as a variable resistance simulator and to apply voltage in dark conditions. The obtained parameters were:

I_m : Electrical current at maximum power point, V_m : Electrical voltage at maximum power point, I_{sc} : Course current circuit ($v=0$), V_{oc} : Open circuit voltage ($I=0$), P_m : Maximum power.

The efficiency (η) was calculated by Eq. 2.

$$\eta = \frac{P_m}{P_{in}} \quad (2)$$

where P_{in} is the solar power that affects the active area, corresponding to $0.13\text{ W}/\text{cm}^2$.

3 Results and discussion

3.1 Fabrication of hydrogel-PANI and NDSSC

Figure 2 shows the ITO-PET substrate with the TiO_2 layer during hydrogel-PANI formation in which UV promoted hydrogel network growth occurred along with PANI polymerization during the contact between a hydrogel precursor solution containing aniline and a solution rich in the initiator (ammonium persulfate). The green colored film is evidence of the formation of a conductive hybrid system. To further elucidate the reaction, the same procedure illustrated in images of Fig. 2 is shown in Fig. 3, in which a large glass vessel was used to accommodate the two solutions and to show the evolution of the hydrogel and PANI formation. The sequence of images shows the formation of PANI at the interface of the two solutions, and its progressive growth towards the hydrogel by diffusion and swelling of the hydrogel promoted by the initiator rich solution. The appearance and flexibility of the final NDSSC, in which another ITO-PET substrate was inserted atop the hydrogel-PANI layer, are shown in Fig. 4.



Fig. 2 ITO-PET substrate with the TiO₂ layer (left) and hydrogel with PANI during polymerization (right)

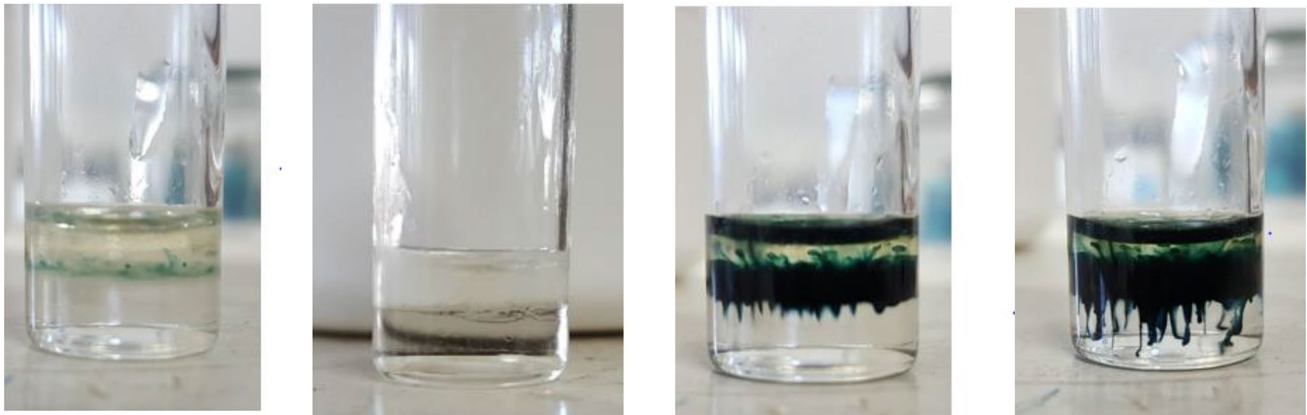


Fig. 3 Sequential events related to polymerization at the interface between Solution B (containing PVA and ammonium persulfate) (lower phase) and Solution A (containing poly(acrylamide-co-acrylic acid) and aniline) (upper phase)



Fig. 4 Final appearance of the NDSSC-containing hydrogel-PANI

3.2 Morphology of hydrogels containing PANI

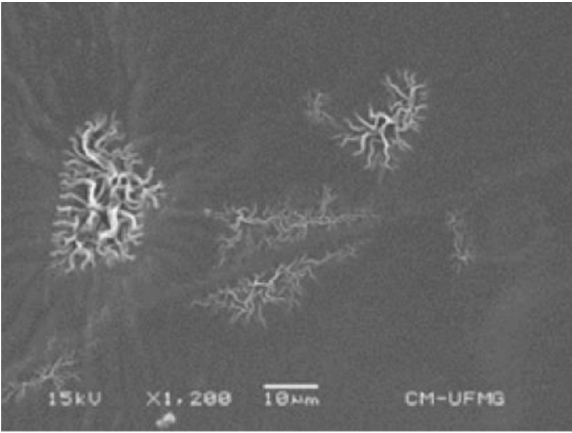
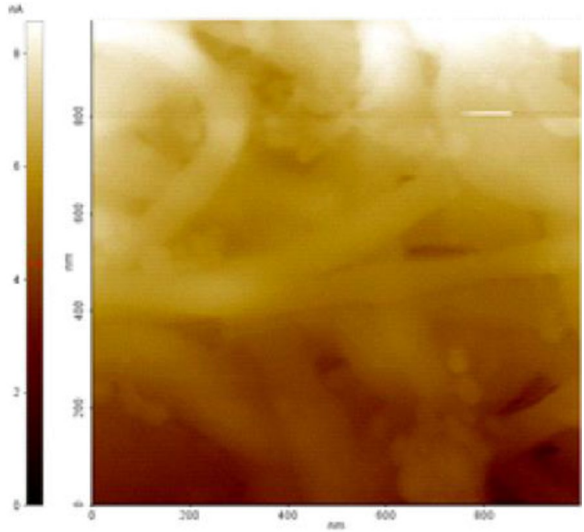
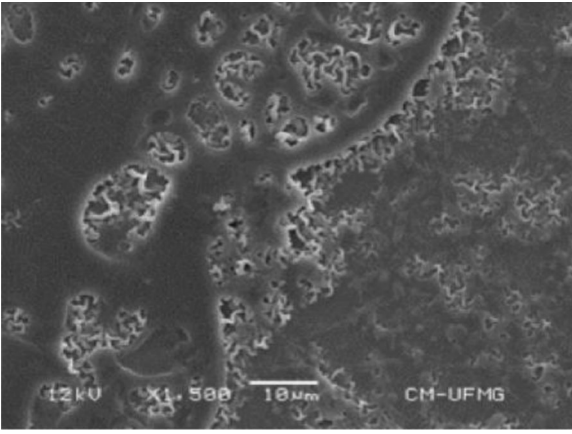
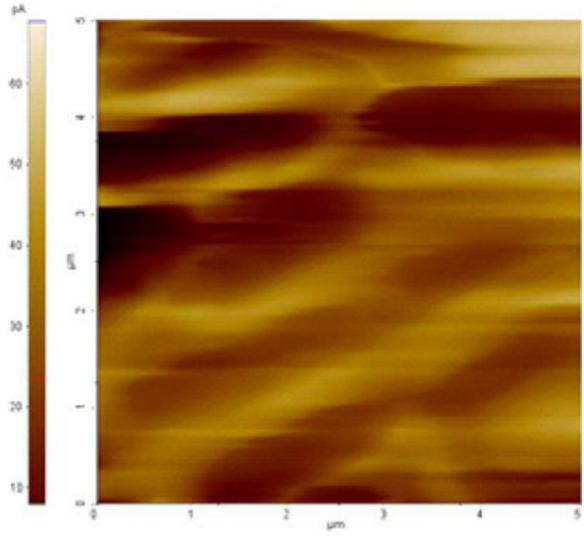
Table 2 shows both SEM and I-AFM (AFM in the conductive mode) images of photopolymerized hydrogel samples containing different amounts of PANI.

The surface of the hydrogel with no PANI (Gel:PANI 0) did not show any major features that could be related to heterogeneities, such as second phases, voids or cracks, which suggests that the UV-promoted polymerization of the hydrogel had occurred as designed. In Gel:PANI 2 samples with the lowest percentages of aniline and

Table 2 SEM and I-AFM images of hydrogel samples with different concentrations of PANI

Sample	SEM image	I-AFM image
Gel:PANI 0		NA
Gel:PANI 2		

Table 2 (continued)

Sample	SEM image	I-AFM image
Gel:PANI 4		
Gel:PANI 6		

ammonium persulfate, it can be clearly observed that the employed synthesis conditions led to a controlled growth of the PANI particles to yield needle-like structures with mean diameter of 70 nm and length of 100–200 nm, as revealed by I-AFM imaging. This special nanostructured morphology is a result of the PANI polymerization confined in a 2D environment, which is represented by the interfacial region in which both viscous solutions interact. Special PANI morphologies due to particular processing conditions have already been observed and reported by others [11]. I-AFM was also useful in confirming that the observed needle-like structures in the SEM image have high electrical conductivity and thus are related to PANI.

SEM and I-AFM images of Gel:PANI 4 and Gel:PANI 6 with increased concentrations of PANI with respect to Gel:PANI 2 show the same trend, in which controlled polymerization growth of the conducting polymer led to special morphologies due to the presence of particular environments, such as the interface of the two precursor solutions and the hydrogel structure, that act as templates for the polymerization of PANI. I-AFM images of Gel:PANI 2, Gel:PANI 4 and Gel:PANI 6 show that higher concentrations of aniline led to shifts in morphology of the PANI phases from needle-like (nanosticks) to long fibers/ribbons and sheets (for the Gel:PANI 6).

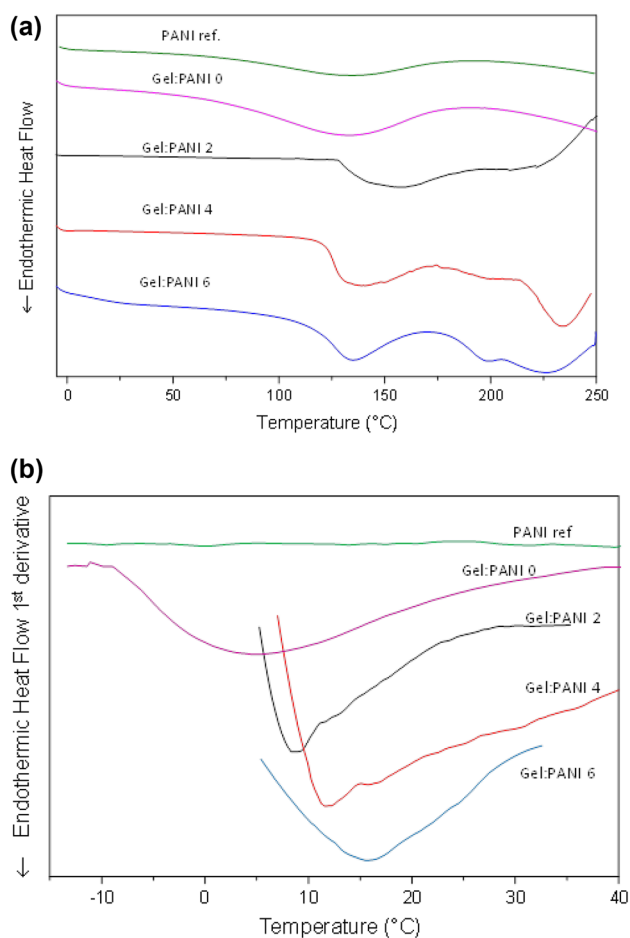


Fig. 5 **a** DSC curves of hydrogels containing different amounts of PANI. **b** First derivative of the DSC curves

3.3 Characterization of hydrogels containing PANI

In Fig. 5, DSC curves of hydrogels containing 2, 4 and 6 wt% PANI are shown together with the DSC curve of commercially available Emerald-type PANI: HCl.PANI as reference (Sigma-Aldrich, St. Louis, MO, USA).

The DSC curve of the commercially available PANI in Fig. 5a shows the typical behavior of the material [12], displaying an endothermic event between 125 and 150 °C corresponding to the loss of the HCl dopant of the material and the start of polymer degradation above 250 °C. In hydrogel samples with PANI, this endothermic event associated with the loss of the HCl dopant shifted to higher temperatures, which indicates that interactions between acrylic acid moieties and PANI would require higher levels of energy to extract the dopant from the PANI structure.

The first derivatives of DSC curves are shown in Fig. 5b to reveal the glass transition temperatures (T_g) (according to ASTM E1356–08) of the hydrogels, which is approximately 5 °C. The T_g of PANI could not be observed due

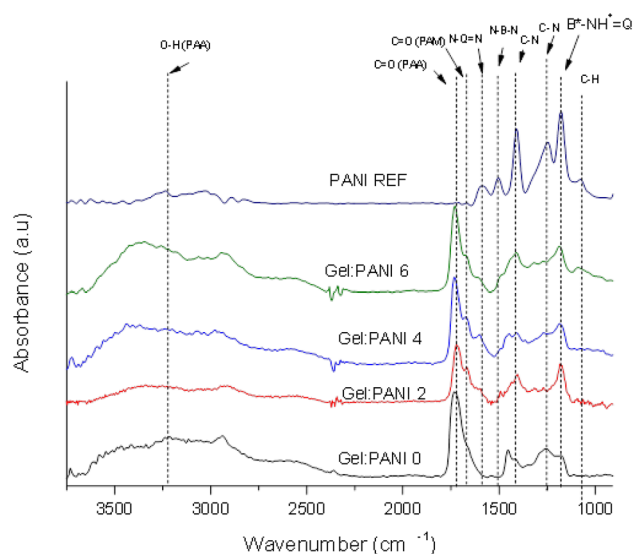


Fig. 6 FTIR spectra of hydrogels with different PANI contents as well as neat PANI as a reference material

to the presence of highly aromatized chains. In Fig. 5b, the relationship between the increase in the percentage of PANI and higher T_g values can be observed: Gel:PANI 2, Gel:PANI 4 and Gel:PANI 6 presented glass transition temperatures of 9, 12 and 16 °C, respectively. This finding confirms that the interactions between the hydrogel and the conductive polymer reduce the overall mobility of the hydrogel chains and function like physical cross-links [13].

3.4 FTIR and UV–Vis spectroscopy results

FTIR spectra of hydrogels and of the commercially available PANI are shown in Fig. 6. The following FTIR bands are typical of PANI: the band at 1600 cm^{-1} , assigned to $\text{N}=\text{Q}=\text{N}$ structures, in which Q represents the quinoid ring; and the $\text{N}-\text{B}-\text{N}$ band at 1496 cm^{-1} , in which B indicates the benzoid ring; and the $\text{B}-\text{NH}^+=\text{Q}$ structure representing the doped structure of the emeraldine PANI [14] at 1155 cm^{-1} and are clearly observed in the spectrum of the commercially available material. These bands can also be observed in the spectra of hydrogels containing PANI. All hydrogel samples showed a distinct absorption band related to carbonyl bonds close to 1724 cm^{-1} that is present in both acrylic acid and acrylamide.

The relative intensity of the $\text{C}=\text{O}$ stretch band of the hydrogel in respect to PANI bands was reduced for samples with higher concentrations of PANI incorporation as evidence of the presence of PANI in these samples. A shift of the $\text{C}=\text{O}$ peak of the hydrogel to lower wavenumbers was also observed, which indicates a strong interaction with PANI, an effect that has also been observed by other authors [14, 15]. This result together with the DSC results

that showed higher temperatures for the loss of the HCl dopant supports the hypothesis of the secondary doping effect of PANI by acrylic acid units of the hydrogel, as reported by others [14].

The relative intensities between the quinoid (Q1600), benzoid (Q₁₄₉₆) and the electronic absorption of conductive polymer bands (I₁₁₅₅) can be used to evaluate the oxidation state of PANI (Eq. 3) and the level of doping (Eq. 4), following the relationships:

$$R_{ox} = I_{1496}/I_{1600} \quad (3)$$

$$R_d = I_{1155}/I_{1496} \quad (4)$$

where R_{ox} is the oxidation index and R_d is the doping value. The calculated values are shown in Table 3.

All samples had values of R_{ox} near 1, which indicates the dominant presence of polyaniline in its emeraldine phase. The highest doping level (R_d) was observed for the Gel:PANI 02, which is the sample with the lowest concentration of PANI; Gel:PANI 02 displayed PANI as thin needle-like structures (also called: nanosticks) that have the highest surface area/volume ratio, which seem particularly useful for improving the ability to have PANI acid doped.

In Fig. 7, the UV–Vis spectra of hydrogel samples containing different amounts of PANI are shown. The spectra of all samples with PANI showed two characteristic absorption peaks at ~315–342 nm and ~405–442 nm. The absorption peak at ~315–342 nm can be ascribed to the π - π^* transition of the benzenoid rings, while the peak at 405–442 nm can be attributed to the polaron- π^* transition. However, when an intense free carrier tail cutoff at approximately 1000 nm appears (as in the case of hydrogels with higher concentrations of PANI), this absorption in the near infrared region can serve as evidence for the delocalization of electrons in the polaron band of the “expanded coil,” which is another strong indication of the secondary-doping-induced conformational transition due to the acrylic acid-PANI interaction and doping [16].

3.5 Nanoindentation measurements

Flexible solar cells and other applications linked to hydrogels would rely on tough hydrogels to withstand designed operations. Mechanical properties of the hydrogels containing PANI both in dry and wet (i.e., underwater)

Table 3 Oxidation index (R_{ox}) and doping values (R_d) for films

Samples	$R_{ox} = I_{1496}/I_{1600}$	$R_d = I_{1155}/I_{1496}$
Gel:PANI 02	1.02 ± 0.06	1.34 ± 0.09
Gel:PANI 04	0.82 ± 0.10	1.09 ± 0.12
Gel:PANI 06	0.98 ± 0.06	1.17 ± 0.10

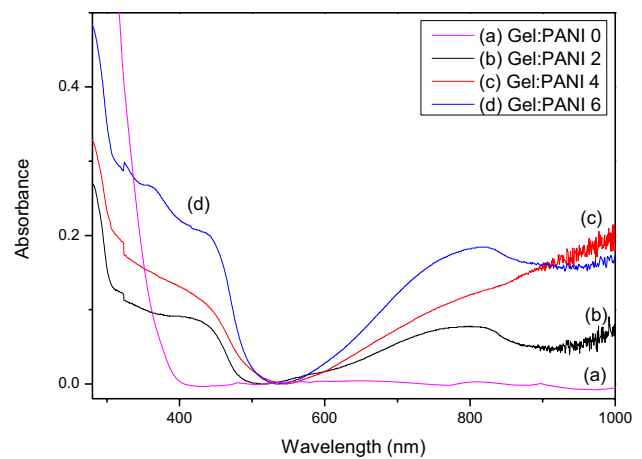


Fig. 7 UV–Vis spectra of hydrogel samples with different amounts of PANI

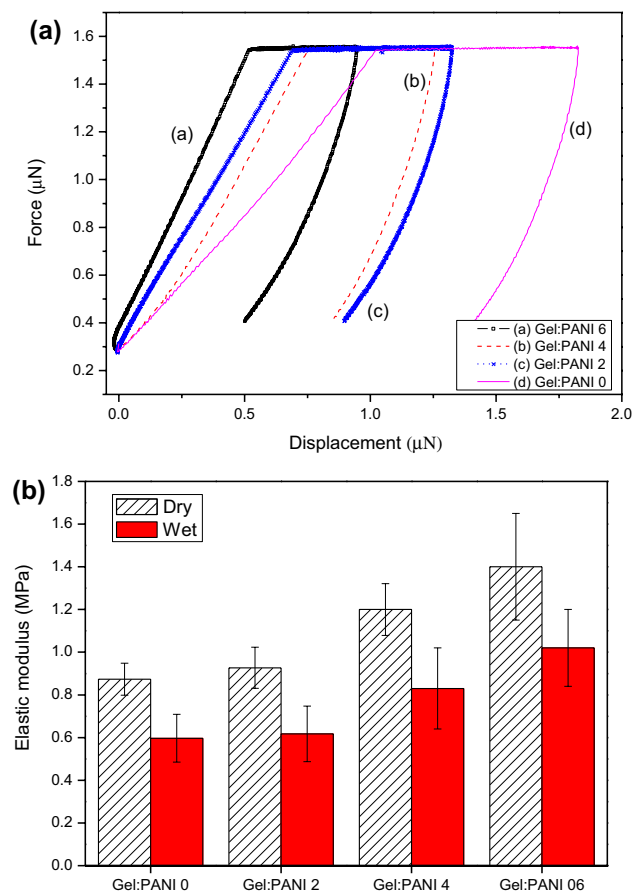


Fig. 8 **a** Force versus displacement measurements related to AFM nanoindentations on hydrogels under water (wet). **b** Elastic modulus values for the different hydrogels containing PANI estimated by AFM nanoindentation measurements

conditions were studied and estimated by using AFM nanoindentation measurements (Fig. 8).

Figure 8a shows force versus displacement curves that were obtained during the nanoindentation measurements. Measurements were performed both in dry and wet conditions (an AFM liquid cell was used for the underwater-wet-measurements). In Fig. 8a, only the underwater measurements for hydrogels with different amounts of PANI are shown for clarity. The results revealed that the incorporation of PANI led to stiffer samples, i.e., for nanoindentation forces of 1.6 μN, the penetration of the AFM tip was much shallower for hydrogels with higher concentrations of PANI.

Results in Fig. 8a were used to estimate the elastic modulus values of the hydrogels, as exhibited in Fig. 8b. As expected, the elastic moduli of swollen (wet) hydrogels were much lower than the elastic moduli for dry hydrogels of the same composition, as a consequence of chain relaxation due to the interaction between water and hydrogel chains. It is also observed in Fig. 8b that the elastic moduli of samples with higher concentrations of PANI were much higher than the modulus of the hydrogel with no PANI (Gel:PANI 0), due to the rigid ring-rich macromolecular structure of PANI, as well as to the intense interactions between PANI and hydrogels that restrict chain mobility and enhance stiffness.

3.6 Electrical conductivity of hydrogels containing PANI

Table 4 reports the overall electrical conductivity of the hydrogel samples with the incorporation of PANI as measured by the 4-point method. The results showed that the incorporation of PANI in the hydrogels led to improvements in the electrical conductivity as expected due to the high electrical conductivity of PANI.

It was observed that the percolation factor was the most significant influence in this type of measurement, since the Gel:PANI 2 sample with the lowest concentration of PANI, in the form of nanosticks, was not able to significantly influence the overall conduction values because the conducting regions of PANI were not interconnected.

Table 4 Conductivity of hydrogel samples with PANI

Sample	Conductivity (S/cm)	Standard deviation (S/cm)
Gel:PANI 2	0.0025	0.0002
Gel:PANI 4	0.0140	0.001
Gel:PANI 6	0.0200	0.005

On the other hand, hydrogel samples with larger amounts of self-assembled PANI nanofibers, such as Gel:PANI 4 and Gel:PANI 6, displayed higher values of conductivity even with low percentages of PANI due to the higher interconnectivity between the conducting regions. The obtained results demonstrated the effectiveness of the developed technique to prepare highly conductive hydrogels containing nanostructured PANI, since conventional PANI blends only tend to have effective conductivity between 10 and 40% PANI content [17].

3.7 Solar cell characterization

In Fig. 9, the voltage–current curves (incident radiation power accounting for the sample size at 130 mW, P_{in}) of NDSSC-type solar cells with quasi-solid electrolytes with inside counter electrodes based on hydrogels containing different amounts of PANI are shown. First, the efficiency values for this type of dye reported in the literature [6, 18] are mostly below 1%, while the highest reported values for *Myrciaria cauliflora* are between 1.1 and 1.6% [19]. Table 5 also reports the values collected during the evaluation of the solar cells and the calculated efficiency.

It can be seen that the open-circuit voltage values of Gel:PANI 4 and GEL:PANI 6 samples are within the range expected in the literature, i.e., a value of approximately 650 mV. On the other hand, short-circuit current and efficiency (> 2%) were higher than the average results reported in the literature, which demonstrates that the hydrogels with the nanostructured PANI were able to reduce current losses by recombination, which usually occurs between oxidation and reduction of iodine ions. This increase in efficiency can be related to the fact that the electrolyte is within the counter electrode in

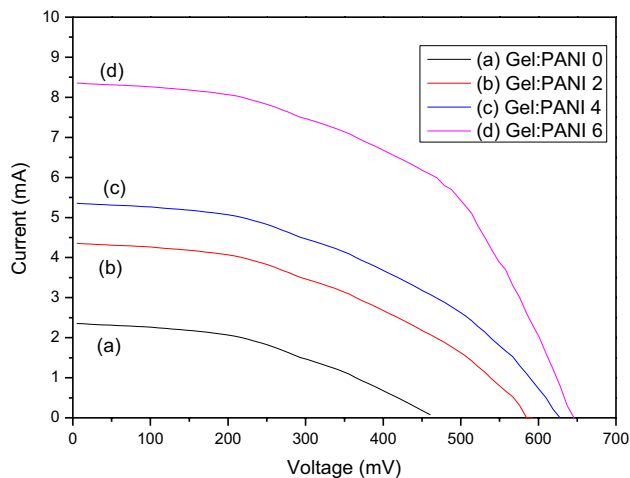
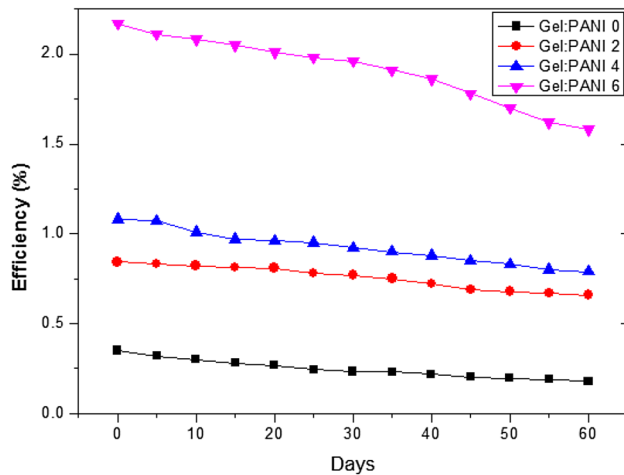


Fig. 9 Voltage–current curves of the samples with incident radiation power

Table 5 Current versus voltage data and efficiency of NDSSC-type solar cells with quasi-solid electrolytes with inside counter electrodes based on hydrogels with different amounts of PANI

Quasi-solid electrolytes	V_{oc} (mV)	I_{sc} (mA cm ⁻²)	V_m (mV)	I_m (mA cm ⁻²)	P_m (mW cm ⁻²)	η (%)	FF
Gel:PANI 0	456	1.77	260	1.35	0.35	0.351	0.44
Gel:PANI 2	580	3.4	356	2.37	0.84	0.843	0.43
Gel:PANI 4	620	4.04	390	2.92	1.14	1.08	0.45
Gel:PANI 6	642	6.39	470	4.61	2.15	2.17	0.53

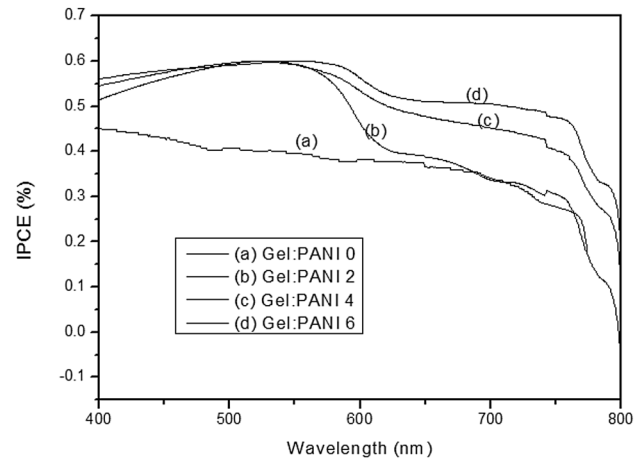
**Fig. 10** DSSCs efficiency as a function of time

the developed NDSSC and, at the same time, the counter electrode also contains nanostructured PANI which is recognized as a powerful catalyst for the reduction of the I_3^- ions. These features of the NDSSC have probably allowed the reduction of the necessary average path of the iodine ions between the TiO_2 layer sensitized with the dye and counter electrode.

In Table 5, values of V_{oc} and I_{sc} can be explained based on the fact that, on charging the material, the electrons are induced and injected from I^- ions into the photo-oxidized dye, and further the produced I^{3-} are reduced on the counter electrode [20]. Therefore, higher contents of PANI inside quasi-solid electrolytes can increase the I^{3-} reduction rate, leading to higher values of I_{sc} . Moreover, charge recombination within the DSSC can also increase the V_{oc} .

Also in Table 5, higher values of fill factor (FF) for samples with high contents of PANI confirmed the tendency of lower resistance in series in comparison with the shunt resistance due to improved generation and transfer of charges to the electrodes.

Figure 10 shows that the presence of PANI in the hydrogels was able to increase the stability of the DSSCs. When hydrogel samples (with no PANI) were used in the DSSCs, a loss of efficiency higher than 50% was noted. Otherwise, a loss of efficiency of less than 30% was observed for DSSCs with hydrogels with PANI (such as Gel:PANI 6),

**Fig. 11** IPCE results of the different DSSCs

as an indication that the quasi-solid electrolytes with PANI were more mechanically stable and were able to restrict the degradation of the dye.

The possibility of having both energy conversion and storage in DSSC containing cations such as Li^+ has been discussed recently [21]. In our case, nanostructured PANI could connect the counter electrodes that would reduce the capacity of storage. Therefore, the DSSCs lifespan may be improved. More studies should be performed to prove it.

IPCE results of the DSSCs are reported in Fig. 11 and show that samples with self-assembled PANI display higher efficiency in the generation and transport of charge carriers due to higher levels of photoabsorption and lower possibility of recombination.

4 Conclusions

In this work, the preparation of hybrid hydrogels, in which a nanostructured PANI was polymerized concomitantly with the formation of the hydrogel network by combining a surface-based polymerization with UV-assisted reaction, was demonstrated. SEM and conductive AFM images showed that the morphology of the PANI phase within the hydrogels shifted from needle-like to fiber-, ribbon- and

sheet-like morphologies when higher concentrations of PANI were used. FTIR, DSC and UV–Vis results indicated that a strong interaction between PANI and the hydrogel chains and a secondary doping of PANI by the acrylic acid moieties were promoted. Nanoindentation measurements demonstrated that PANI was able to enhance the elastic moduli of both wet and dry hydrogels. Moreover, the electrical conductivity of the hydrogels was significantly improved by the incorporation of PANI with low percolation thresholds. Natural dye-sensitized solar cells were fabricated by using the developed hydrogel containing PANI as a quasi-solid electrolyte with inside counter electrode and the shell of *Myrciaria cauliflora* (jaboticaba) as a dye. Solar cell efficiencies above 2% were measured, which indicated that hydrogels containing PANI can act as quasi-solid electrolytes, as well as that counter electrodes can enhance diffusion and reduction of iodine ions. Therefore, hydrogels with nanostructured PANI were shown to be good candidates for quasi-solid electrolytes that can also act as counter electrodes for flexible solar cells, such as those based on natural dye sensitizers.

Acknowledgements The authors acknowledge the financial support from CNPq, Coordenação de Aperfeiçoamento de Pessoal de Nível Superior - Brasil (CAPES, Finance Code 001) and FAPEMIG.

Compliance with ethical standards

Conflict of interest The authors declare that they have no conflict of interest.

References

- Wei D (2010) Dye sensitized solar cells. *Int J Mol Sci* 11:1103–1113. <https://doi.org/10.3390/ijms11031103>
- Al-bahrani MR, Xu X, Ahmad W, Ren X, Su J, Cheng Z, Gao Y (2014) Highly efficient dye-sensitized solar cell with GNS/MWCNT/PANI as a counter electrode. *Mater Res Bull* 59:272–277. <https://doi.org/10.1016/j.materresbull.2014.07.029>
- Kong F-T, Dai S-Y, Wang K-J (2007) Review of recent progress in dye-sensitized solar cells. *Adv Optoelectron* 2007:1–13. <https://doi.org/10.1155/2007/75384>
- Li Q, Tang Q, Chen H, Xu H, Qin Y, He B, Liu Z, Jin S, Chu L (2014) Quasi-solid-state dye-sensitized solar cells from hydrophobic poly(hydroxyethyl methacrylate/glycerin)/polyaniline gel electrolyte. *Mater Chem Phys* 144:287–292. <https://doi.org/10.1016/j.matchemphys.2013.12.032>
- Tang Z, Wu J, Liu Q, Zheng M, Tang Q, Lan Z, Lin J (2012) Preparation of poly(acrylic acid)/gelatin/polyaniline gel-electrolyte and its application in quasi-solid-state dye-sensitized solar cells. *J Power Sour* 203:282–287. <https://doi.org/10.1016/j.jpowsour.2011.11.039>
- Richhariya G, Kumar A, Tekasakul P, Gupta B (2017) Natural dyes for dye sensitized solar cell: a review. *Renew Sustain Energy Rev* 69:705–718. <https://doi.org/10.1016/j.rser.2016.11.198>
- Leyrer J, Hunter R, Rubilar M, Pavez B, Morales E, Torres S (2016) Development of dye-sensitized solar cells based on naturally extracted dye from the maqui berry (*Aristotelia chilensis*). *Opt Mater* 60:411–417. <https://doi.org/10.1016/j.optmat.2016.08.021>
- Amaral RC, Barbosa DRM, Zanoni KPS, Iha NYM (2017) Natural sensitizers for DSCs improved with nano-TiO₂ compact layer. *J Photochem Photobiol A* 346:144–152. <https://doi.org/10.1016/j.jphotochem.2017.05.046>
- Oliver WC, Pharr GM (1992) An improved technique for determining hardness and elastic modulus using load and displacement sensing indentation experiments. *J Mater Res* 7:1564–1583. <https://doi.org/10.1557/jmr.1992.1564>
- Blythe T, Bloor D (2008) Electrical properties of polymers, 2nd edn. Cambridge University Press, Cambridge
- Kumar V, Mahajan R, Bhatnagar D, Kaur I (2016) Nanofibers synthesis of ND:pANI composite by liquid/liquid interfacial polymerization and study on the effect of NDs on growth mechanism of nanofibers. *Eur Polymer J* 83:1–9. <https://doi.org/10.1016/j.eurpolymj.2016.07.025>
- Stejskal J, Gilbert RG (2002) Polyaniline. Preparation of a conducting polymer(IUPAC Technical Report). *Pure Appl Chem* 74:857–867. <https://doi.org/10.1351/pac200274050857>
- Reed EW (2010) Synthesis of a directionally-conductive polyaniline hydrogel composite by vapor deposition, Master Thesis University of Louisville
- Xu LL, Shahid S, Patterson DA, Emanuelsson EAC (2019) Flexible electro-responsive in situ polymer acid doped polyaniline membranes for permeation enhancement and membrane fouling removal. *J Membr Sci* 578:263–272. <https://doi.org/10.1016/j.memsci.2018.09.070>
- Xia Y, Zhu H (2011) Polyaniline nanofiber-reinforced conducting hydrogel with unique pH-sensitivity. *Soft Matter* 7:9388. <https://doi.org/10.1039/c1sm05890h>
- Athawale AA, Kulkarni MV, Chabukswar VV (2002) Studies on chemically synthesized soluble acrylic acid doped polyaniline. *Mater Chem Phys* 73:106–110. [https://doi.org/10.1016/s0254-0584\(01\)00338-8](https://doi.org/10.1016/s0254-0584(01)00338-8)
- Mittal V (2017) Functional polymer blends: synthesis properties and performance. CRC Press, Boca Raton
- Hug H, Bader M, Mair P, Glatzel T (2014) Biophotovoltaics: natural pigments in dye-sensitized solar cells. *Appl Energy* 115:216–225. <https://doi.org/10.1016/j.apenergy.2013.10.055>
- Polo A, Murakamiha N (2006) Blue sensitizers for solar cells: natural dyes from Calafate and Jaboticaba. *Sol Energy Mater Sol Cells* 90:1936–1944. <https://doi.org/10.1016/j.solmat.2006.02.006>
- Dao V-D, Kim S-H, Choi H-S, Kim J-H, Park H-O, Lee JK (2011) Efficiency enhancement of dye-sensitized solar cell using pt hollow sphere counter electrode. *J Phys Chem C* 115:25529–25534. <https://doi.org/10.1021/jp208295b>
- Dao V-D (2017) Comment on “energy storage via polyvinylidene fluoride dielectric on the counter electrode of dye-sensitized solar cells”. *J Power Sour* 337:125–129. <https://doi.org/10.1016/j.jpowsour.2016.10.100>

Publisher's Note Springer Nature remains neutral with regard to jurisdictional claims in published maps and institutional affiliations.